Robust Performance of AlGaN-Channel Metal-Insulator-Semiconductor High-Electron-Mobility Transistors at High Temperatures *

Li Zhang(张力), Jin-Feng Zhang(张金风), Wei-Hang Zhang(张苇杭), Tao Zhang(张涛), Lei Xu(徐雷), Jin-Cheng Zhang(张进成)**, Yue Hao(郝跃)

Key Lab of Wide Band-Gap Semiconductor Technology, School of Microelectronics, Xidian University, Xi'an 710071

(Received 3 July 2017)

Superior characteristics of AlGaN-channel metal-insulator-semiconductor (MIS) high electron mobility transistors (HEMTs) at high temperatures are demonstrated in detail. The temperature coefficient of the maximum saturation drain current for the AlGaN-channel MIS HEMT can be reduced by 50% compared with the GaN-channel HEMT. Moreover, benefiting from the better suppression of gate current and reduced leakage current in the buffer layer, the AlGaN-channel MIS HEMT demonstrates an average breakdown electric field of 1.83 MV/cm at 25°C and 1.06 MV/cm at 300°C, which is almost 2 times and 3 times respectively larger than that of the reference GaN-channel HEMT. Pulsed mode analyses suggest that the proposed device suffers from smaller current collapse when the temperature reaches as high as 300°C.

PACS: 85.30.Tv, 72.80.Ey, 85.30.De DOI: 10.1088/0256-307X/34/12/128501

GaN-channel high electron mobility transistors (HEMTs) are competitive candidates for future high power and high frequency applications and various superior characteristics have been reported by many research groups.[1–4] To meet the daily increasing requirement of the high-power application, the HEMT using AlGaN as channel material which has a wider band gap than GaN was proposed to demonstrate the breakdown voltage enhancement.[5] Nanjo *et al.* reported the maximum breakdown voltage of 1650 V with heterostructure of $Al_{0.53}Ga_{0.47}N/Al_{0.38}Ga_{0.62}N$.[6] Meanwhile, Stroke *et al.* reported favorable characteristics of the AlGaN-channel HEMT on an AlN substrate, and the breakdown voltage of 1800 V was achieved.[7]

Since the junction temperature of GaN-based devices during applications is very high, it is necessary to study devices operated at high temperature due to self-heating effect.[8] However, there are few reports on breakdown characteristics at high temperature. In this work, the temperature-dependent electrical characteristics of AlGaN-channel MIS HEMTs have been systematically studied by I–V, C–V, off-state breakdown and pulsed mode measurement.

The structure (sample A) used in this study consists of mainly a 22 nm $Al_{0.40}Ga_{0.60}N$ barrier layer and a 1 μm $Al_{0.18}Ga_{0.82}N$ buffer layer, grown on a 2-in c-plane sapphire substrate (Fig. 1(a)) For comparison, a reference HEMT (sample B) based on the conventional $Al_{0.30}Ga_{0.70}N$ (22 nm)/GaN (2000 nm) heterojunction is shown in Fig. 2(b). Sample A fabrication started from the mesa isolation, then the Ti/Al/Ni/Au was evaporated by e-beam evaporator and alloyed at 830℃ for 30 s by rapid thermal annealing (RTA) as ohmic contacts. After the deposition of a 10 nm SiN_x insulating layer, the Ni/Au gate electrodes were formed. Sample B was fabricated by the same process as sample A except for deposition of the SiN_x dielectric layer. Lastly, it became completed by the deposition of a 10 nm SiN_x insulator layer. Both the devices exhibit a gate width of 50 μm, a gate length (L_G) of 1 μm, a source–gate spacing (L_{GS}) of 1 μm, and a gate–drain (L_{GD}) spacing of 1 μm.

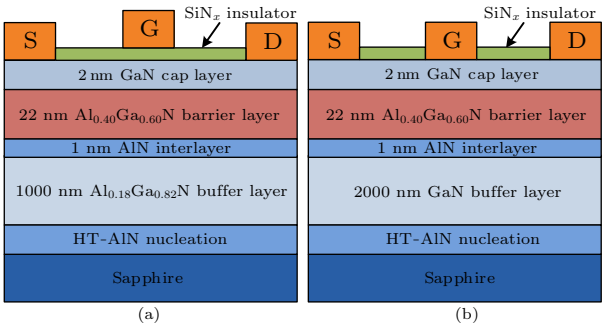

Fig. 1. Schematic structures of (a) the $Al_{0.40}Ga_{0.60}N/Al_{0.18}Ga_{0.82}N$ MIS HEMT and (b) the $Al_{0.30}Ga_{0.70}N/GaN$ HEMT.

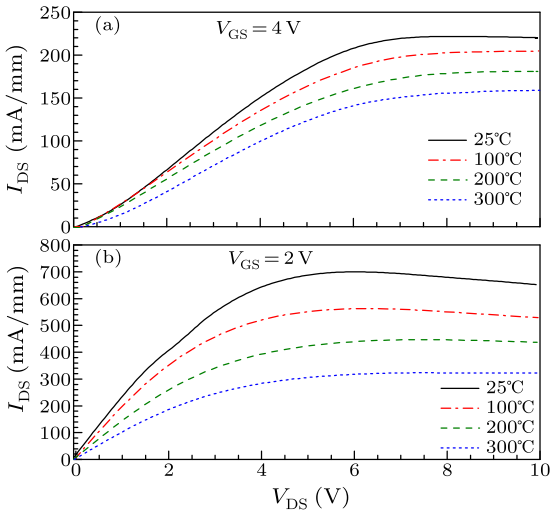

Fig. 2. Output characteristics at different temperatures of (a) sample A and (b) sample B.

*Supported by the 111 Project (B12026).
**Corresponding author. Email: jchzhang@xidian.edu.cn
© 2017 Chinese Physical Society and IOP Publishing Ltd

The high-temperature output characteristics of both the samples are shown in Fig. 2, and a gradual decrease in the maximum saturation drain current ($I_{\rm Dsat}$) with increasing temperature is observed. For sample A, $I_{\rm Dsat}$ decreases by about 27% from 220 mA/mm at 25℃ to 161 mA/mm at 300℃. When it comes to sample B, $I_{\rm Dsat}$ decreases significantly from 667 mA/mm at 25℃ to 312 mA/mm at 300℃, corresponding to about 53% degradation, which is twice as large as sample A.

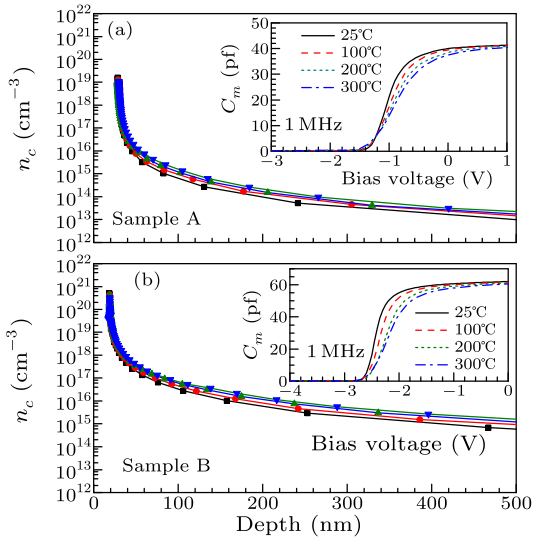

Fig. 3. Temperature-dependent depth profiles of electrons of (a) $Al_{0.40}Ga_{0.60}N/Al_{0.18}Ga_{0.82}N$ diode and (b) conventional AlGaN/GaN diode. The C–V curves at different temperatures for the two diodes are shown in the insets.

It is known that the different current degradations are strongly related to the different channel properties of HEMTs. Here the characteristics of AlGaN channel and GaN channel are evaluated by testing the temperature-dependent C–V of the Schottky diodes. According to the test results on diode for sample A (inset of Fig. 3(a)) and diode for sample B (inset of Fig. 3(b)), the depth profiles of electrons under the gate are derived (Fig. 3) according to[9,10]

$$Z = \frac{\varepsilon A}{C}, \tag{1}$$

$$n_{\rm c} = -\frac{2}{e\varepsilon A^2} \cdot \frac{1}{d(1/C^2)/dV} q, \tag{2}$$

where Z is the depth to gate, ε is the dielectric constant of barrier, C is the junction capacitor, and A is the area of junction capacitor. The material constants used in this study are $\varepsilon_{\rm r,SiN} = 7.2$, $\varepsilon_{\rm r,Al0.4GaN} = 8.66$, and $\varepsilon_{\rm r,Al0.3GaN} = 8.78$.[11]

For both diodes, the slope of C–V curves is becoming gentler as the temperature increases, which is probably due to the poor confinement of the two-dimensional electron gas (2DEG). The electrons overflow from the potential well and become trapped in the barrier and buffer, leading to the reduction of 2DEG density in the channel and even a more dispersed distribution of carrier.[12] In addition, due to the low polarization intensity between $Al_{0.4}GaN$ barrier and $Al_{0.18}GaN$ channel, the channel carrier density of sample A is lower than that of sample B. Wider band gap of AlGaN buffer reduces the ionization rate of impurity, which effectively suppresses the carrier density.[13]

The 2DEG sheet density $n_{\rm s}$ approximated by $n_{\rm s} = \int_{-\infty}^{+\infty} n_{\rm c}(Z)dZ$ (Fig. 4(a)) changes from $5.68 \times 10^{12}\,{\rm cm}^{-2}$ at 25℃ to $4.94 \times 10^{12}\,{\rm cm}^{-2}$ at 300℃ for sample A, and from $8.54 \times 10^{12}\,{\rm cm}^{-2}$ at 25℃ to $7.64 \times 10^{12}\,{\rm cm}^{-2}$ at 300℃ for sample B. The decrease of $n_{\rm s}$ with temperature is mainly due to the reduction of conduction band discontinuity ($\Delta E_{\rm c}$) of AlGaN/(Al)GaN heterojunctions.[14] Channel mobility (Fig. 4(b)) is also calculated according to[15] $\rho = 1/qn_{\rm s}\mu$ with the sheet resistance ($R_{\rm sh}$) extracted from TLM measurement. Mobility degradations of 60% and 82% for samples A and B can be observed respectively. The significantly reduced temperature-dependent mobility of sample A can be ascribed to lower acoustic and optical phonon scattering of AlGaN channel at high temperature.[16] Thus the relatively better maintenance $I_{\rm Dsat}$ of sample A at elevated temperature is mainly determined by the degradation of the channel mobility.

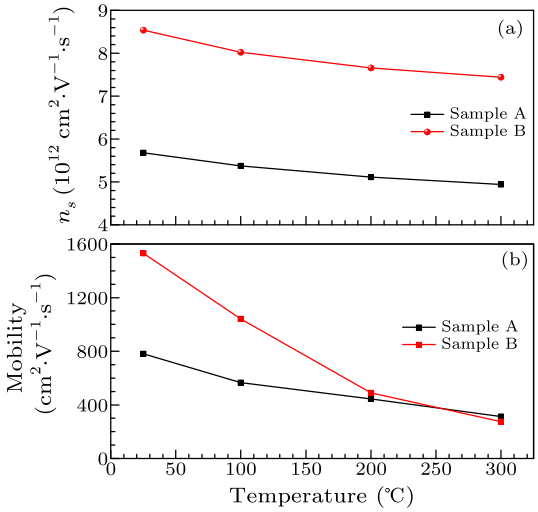

Fig. 4. (a) Calculated 2DEG density and (b) channel mobility for both the samples.

Three-terminal measurement at different temperatures is carried out to study the off-state breakdown characteristics of both the samples. The devices with 1 μm $L_{\rm GD}$ are measured at the gate voltage ($V_{\rm GS}$) of −5 V with the source grounded. The breakdown voltage ($V_{\rm BR}$) is defined as the voltage when the drain current reaches 1 mA/mm and the results are shown in Fig. 5.

From Fig. 5(a), a very high $V_{\rm BR}$ of 183 V for sample A can be seen, which means that the average breakdown electric field ($E_{\rm BR}$) reaches 1.83 MV/cm. When it comes to sample B, the results show a $V_{\rm BR}$ of 91 V and a $E_{\rm BR}$ of 0.91 MV/cm at room temperature. It is clear that $V_{\rm BR}$ of both the devices decreases with increasing temperature, which is from 183 V at 25℃

to 106 V at 300℃ for sample A and from 91 V at 25℃ to 36 V at 300℃ for sample B.

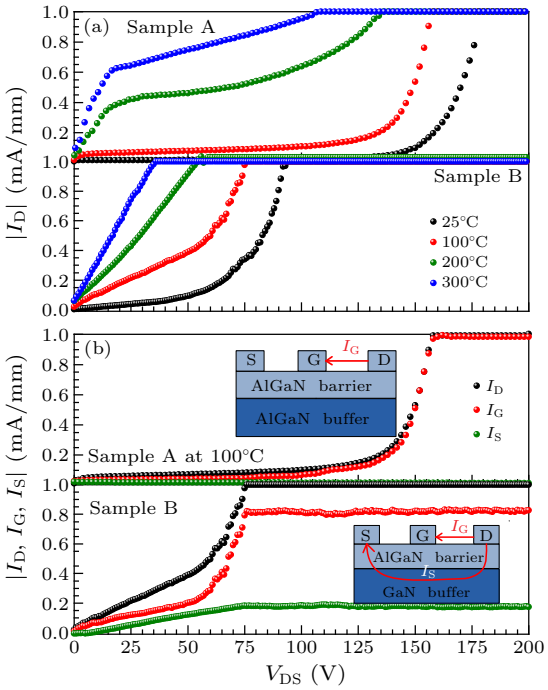

Fig. 5. Off-state characteristic of both the samples (a) at different temperatures and (b) at 100℃. The insets show the different compositions of I_D for samples A and B.

On the other hand, Fig. 5(b) plots the drain current I_D, gate leakage current I_G and source current I_S of both the devices at 100℃. Evidently, I_D is mainly contributed by I_G for both the samples, thus benefiting from the AlGaN channel and the SiN insulator.[17] Sample A shows suppressed I_G and higher E_{BR}. What is more, from the depth profiles of electrons shown in Fig. 3, the background carrier density in sample B is two orders of magnitude higher than sample A, which causes the higher I_S in sample B. The insets also show the different compositions of I_D for samples A and B, where I_D and I_G refer to the current through the gate electrode and the source electrode, respectively. Thus due to the suppressed gate leakage current and reduced leakage current in the buffer layer induced by lower background carrier density extracted from C–V measurement, sample A obtains much higher V_{BR} and E_{BR} at both room temperature and high temperature.[18]

The degradations in the operation of pulsed mode I–V known as current collapse are further investigated. Pulse I_{DS}–V_{DS} results of samples A and B at room temperature are shown in Fig. 6. The pulse-mode measurements are characterized on a quiescent gate bias point (V_{GQ}) of −5 V and drain bias point (V_{DQ}) of 10 V with a pulse width of 500 ns and a pulse period of 1 ms. The exposure to high drain bias in the off-state results in a significant decrease in drain current in both the samples, which is known to be caused by electrons trapped at the surface defects during the off-state.[19] Obviously, a difference of channel layer structure does not affect the current collapse, as similar curves in pulsed mode are obtained in both the HEMTs. Therefore, current collapse is considered to be induced by the similar mechanism in the two HEMTs.

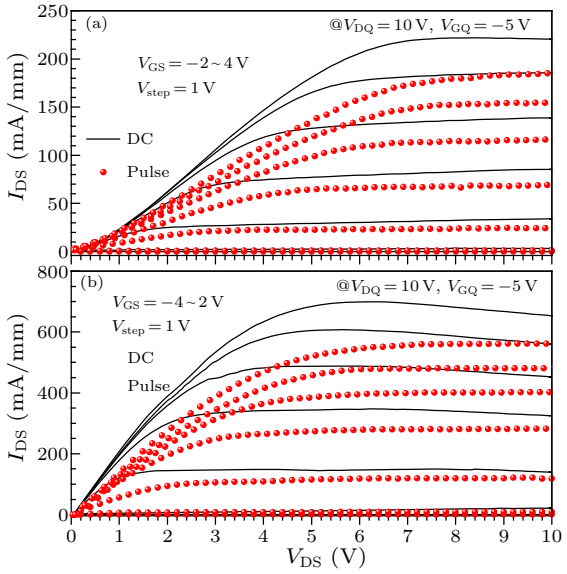

Fig. 6. The dc and pulse I_D–V_D curves of (a) sample A and (b) sample B at room temperature.

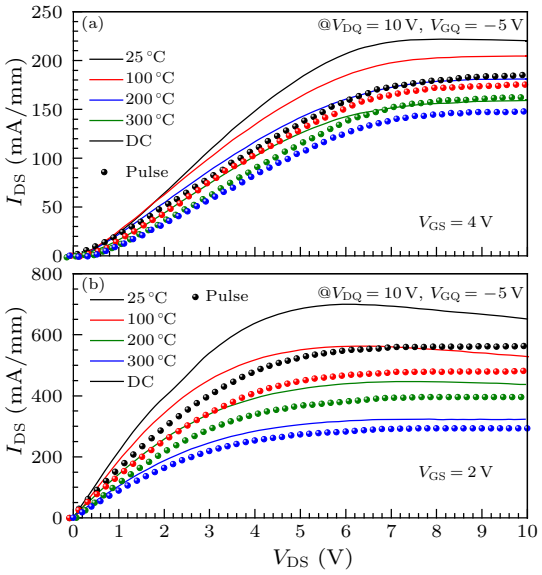

Fig. 7. The dc and pulse I_D–V_D curves of (a) sample A and (b) sample B at different temperatures.

Figure 7 shows the current collapse of both the samples at different temperatures. The most serious current collapse occurs at room temperature. Then, with the increase of temperature, the current collapse effect is weakened, which can be ascribed to reduction of trap time constant as reported in many GaN-based HEMTs.[20] When the temperature reaches 300℃, the amount of current collapse can be suppressed to 8% and 5% for samples A and B, respectively.

In summary, temperature-dependent electrical characteristics of AlGaN-channel MIS HEMT have

been systematically studied in a wide temperature range from 25℃ to 300℃. The results indicate that due to weaker degradation of the channel mobility, the proposed device shows significantly reduced temperature-dependent $I_{\rm Dsat}$ compared with conventional AlGaN/GaN HEMTs. Also, much higher breakdown electric fields of 1.83 MV/cm at 25℃ and 1.06 MV/cm at 300℃ have been observed, which can be ascribed to the suppression of gate leakage current and reduced leakage current in the buffer layer. Additionally, pulsed mode measurement at different temperatures reveals that the current collapse effect is weakened with the increase of temperature due to the reduction of trap time constant. These results indicate that the AlGaN-channel MIS HEMT is very promising for high-performance device applications at high temperatures.

References

[1] Zhang K, Cao M Y, Lei X Y, Zhao S L, Yang L Y, Zheng X F, Ma X H and Hao Y 2013 *Chin. Phys.* B **22** 097303
[2] Chu F T, Chen C, Zhou W and Liu X Z 2013 *Chin. Phys. Lett.* **30** 097303
[3] Quan S, Ma X H, Zheng X F and Hao Y 2013 *Chin. Phys. Lett.* **30** 028503
[4] Wang Y, Yu N S, Li M and Lau K M 2011 *Chin. Phys. Lett.* **28** 057102
[5] Li X D, Zhang J C, Zou Y, Ma X Z, Liu C, Zhang W H, Wen H J and Hao Y 2015 *Chin. Phys. Lett.* **32** 077205
[6] Nanjo T, Takeuchi M, Suita M, Abe Y, Oishi T and Tokuda Y 2008 *Appl. Phys. Express* **1** 011101
[7] Stroke G W and Halioua M 1972 *Phys. Lett.* A **39** 269
[8] Vitanov S, Palankovski V, Maroldt S and Quay R 2010 *Solid-State Electron.* **54** 1105
[9] Arulkumaran S, Egawa T, Ishikawa H and Jimbo T 2002 *Appl. Phys. Lett.* **80** 2186
[10] Krispin P, Spruytte S G, Harris J S and Ploog K H 2000 *J. Appl. Phys.* **88** 4153
[11] Levinshtein M E, Rumyantsev S L and Shur M S 2008 *Properties of Advanced Semiconductor Materials: GaN, AlN, InN, BN, SiC, SiGe* (New York: Wiley)
[12] Maeda N, Tsubaki K, Saitoh T and Kobayashi N 2001 *Appl. Phys. Lett.* **79** 1634
[13] Simon J, Protasenko V, Lian C, Xing H and Jena D 2010 *Science* **327** 60
[14] Zhang J F, Wang C, Zhang J C and Hao Y 2006 *Chin. Phys.* B **15** 1060
[15] Albert G, Andrew M, Erica A, Carlos A, Michael P, Michael E, Torben R and Robert J 2016 *Appl. Phys. Lett.* **109** 033509
[16] Ulek R T, Ligaz A, Okden S G, Teke A, zturk M O, Kasap M, Czelik S O, Arsian E and Zbay E O 2009 *J. Appl. Phys.* **105** 013707
[17] Yagi S, Shimizu M, Inada M, Yamamoto Y, Piao G and Okumura H 2006 *Solid-State Electron.* **50** 1057
[18] Eldad B T, Hilt O, Brunner F, Wurfl J and Trankle G 2008 *IEEE Trans. Electron Devices* **55** 3354
[19] Vetury R, Zhang N Q, Keller S and Mishra U K 2001 *IEEE Trans. Electron Devices* **48** 560
[20] Meneghesso G, Verzellesi G, Pierobon R and Rampazzo F 2004 *IEEE Trans. Electron Devices* **51** 1554